Charge-changing cross sections of ^{30}Ne, ^{32,33}Na with a proton target

A. Ozawa,[1] T. Moriguchi,[1] T. Ohtsubo,[2] N. Aoi,[3] D. Q. Fang,[4] N. Fukuda,[3] M. Fukuda,[5] H. Geissel,[6] I. Hachiuma,[7] N. Inabe,[3]
Y. Ishibashi,[1] S. Ishimoto,[8] Y. Ito,[1] T. Izumikawa,[9] D. Kameda,[3] T. Kubo,[3] T. Kuboki,[7] K. Kusaka,[3] M. Lantz,[3] Y. G. Ma,[4]
M. Mihara,[5] Y. Miyashita,[10] S. Momota,[11] D. Nagae,[1] K. Namihira,[7] D. Nishimura,[5] H. Ooishi,[1] Y. Ohkuma,[2] T. Ohnishi,[3]
M. Ohtake,[3] K. Ogawa,[1] Y. Shimbara,[12] T. Suda,[3] T. Sumikama,[10] H. Suzuki,[1] S. Suzuki,[2] T. Suzuki,[6] M. Takechi,[3] H. Takeda,[3]
K. Tanaka,[3] R. Watanabe,[2] M. Winkler,[6] T. Yamaguchi,[7] Y. Yanagisawa,[3] Y. Yasuda,[1] K. Yoshinaga,[10]
A. Yoshida,[3] and K. Yoshida[3]

[1]*Institute of Physics, University of Tsukuba, Ibaraki 305-8571, Japan*
[2]*Department of Physics, Niigata University, Niigata 950-2181, Japan*
[3]*RIKEN, Nishina Center, Wako, Saitama 351-0198, Japan*
[4]*Shanghai Institute of Applied Physics, Chinese Academy of Sciences, Shanghai 201800, People's Republic of China*
[5]*Department of Physics, Osaka University, Osaka 560-0043, Japan*
[6]*Gesellschaft für Schwerionenforschung GSI, 64291 Darmstadt, Germany*
[7]*Department of Physics, Saitama University, Saitama 338-8570, Japan*
[8]*High Energy Accelerator Research Organization (KEK), Ibaraki 305-0801, Japan*
[9]*RI Center, Niigata University, Niigata 950-2102, Japan*
[10]*Department of Physics, Tokyo University of Science, Tokyo 278-8510, Japan*
[11]*Faculty of Engineering, Kochi University of Technology, Kochi 782-8502, Japan*
[12]*Graduate School of Science and Technology, Niigata University, Niigata 950-2181, Japan*

The total charge-changing, charge pick-up, and partial charge-changing cross sections of very neutron-rich nuclei (^{30}Ne, ^{32,33}Na) with a proton target have been measured at $\sim$240A MeV for the first time. We introduced the phenomenological correction factor in Glauber-model calculations for the total charge-changing cross sections with the proton target, and applied it to deduce the proton radii of these nuclei. For ^{30}Ne and ^{32}Na, the neutron skin thicknesses of the nuclei were deduced by comparing the proton radii with the matter radii deduced from the interaction cross-section measurements. A significant thick neutron-skin has been observed for the nuclei. We also found that the charge pick-up cross sections are much larger than those in the systematics of stable nuclei.

I. INTRODUCTION

The total charge-changing cross sections σ_{cc}, which are the total cross sections where incident nuclei change their charge Z, charge pick-up cross sections $\sigma_{\Delta Z=+1}$, and partial charge-changing cross sections $\sigma_{\Delta Z=-1,-2,\ldots}$ of energetic heavy ions are of interest for various research fields. Systematic measurements allow one to develop models and empirical formulas to predict the cross sections. These models and formulas are applied to study radiation protection issues, including radiation shields for accelerators, reactors, and spacecraft, and in heavy-ion cancer therapy [1]. These cross sections are also important to understand the origin, acceleration mechanism, and propagation of high-energy galactic cosmic rays. A number of systematic measurements were performed using various energy ranges of ions on various targets in the stable nuclei region [2–4]. However, it is unclear whether the models and empirical formulas deduced in the stable nuclei region hold in the unstable nuclei region. Thus, measurements of σ_{cc}, $\sigma_{\Delta Z=+1}$, and $\sigma_{\Delta Z=-1,-2,\ldots}$ for unstable nuclei are important. Especially, the measurements of σ_{cc}, $\sigma_{\Delta Z=+1}$, and $\sigma_{\Delta Z=-1,-2,\ldots}$ for unstable nuclei with a proton target are very rare, and are thus interesting.

In peripheral collisions, σ_{cc} may reflect the collision probability of the valence proton(s) of the projectile with the target nucleus in a simple picture, and thus may be sensitive to the (point-)proton distribution, particularly for neutron-rich projectiles. Chulkov *et al*. measured σ_{cc} for neutron-rich unstable nuclei from boron to fluorine isotopes at a relativistic energy on carbon targets at GSI [5]. They found that σ_{cc} stays constant among the isotopes in each element. Since their nuclear matter radii increase toward the neutron drip line, the data suggest that only the valence neutrons that are added to the core nuclei contribute to enlarging the matter radii, and the proton distributions remain unperturbed even near the neutron drip line. Bochkarev *et al*. also found evidence for the neutron skin in ^{20}N using a combined analysis of the interaction and charge-changing cross sections [6]. Their analysis, however, only gives the upper limit of the radius for the proton distribution. Recently, based on Glauber-model calculations, Yamaguchi *et al*. succeeded to relate the root-mean-square (RMS) proton radius r_p from σ_{cc} by introducing a phenomenological correction factor in the carbon target [7]. They applied the correction factor to deduce the unknown r_p for ^{15,16}C and finally deduced the neutron skin thicknesses for these nuclei [8]. This application is very valuable to deduce r_p of unstable nuclei. Isotope-shift measurements have so far provided the highest precision for the charge radii of unstable nuclei. Also, electron-scattering experiments on unstable nuclei are under way at radioactive ion-beam facilities worldwide [9,10]. However, both methods have certain limitations concerning their applicability, mainly
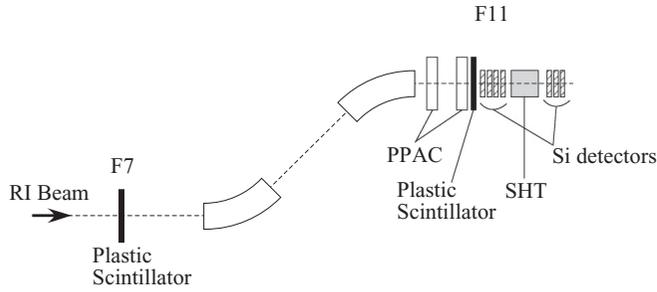
FIG. 1. Experimental setup in the zero-degree spectrometer (ZDS) at the RI-beam factory (RIBF) at the end of the Big-RIPS.

due to a low luminosity of rare isotopes close to the neutron drip line. On the other hand, measurements of σ_{cc} and interaction cross section σ_I, which are the cross sections where the incident nuclei change their mass number A and/or Z, have no limits in the isotopes, and both can be applied to nuclei located very far from stability. Thus, by this new method it may be possible to deduce the skin thickness for nuclei very neutron and/or proton rich. The deduced skin information will provide a definitive description concerning the equation-of-state for neutron-rich nuclei [11]. At this moment, it is unclear whether this new method to deduce r_p from σ_{cc} can be applied to whole nuclei in the nuclear chart, or even for other target cases. In the present work, we measured σ_{cc} for neutron-rich ^{30}Ne, ^{32,33}Na with the proton target, and applied this new method to deduce r_p from σ_{cc} for these nuclei. Finally, we successfully deduced r_p for these nuclei.

II. EXPERIMENTS AND ANALYSIS

Experiments were performed at the RI-beam factory (RIBF) operated by the RIKEN Nishina Center and the Center for Nuclear Study, University of Tokyo. A primary beam of $345A$ MeV ^{48}Ca with a typical intensity of 100 pnA and Be production targets was used to produce ^{30}Ne, ^{32,33}Na secondary beams. The experimental setup for the measurements of σ_{cc}, $\sigma_{\Delta Z=+1}$, and $\sigma_{\Delta Z=-1,-2,\dots}$ with the proton target is shown in Fig. 1. Secondary beams have been produced and separated in Big-RIPS [12], and transported to the zero-degree spectrometer (ZDS) [12]. The secondary beams were irradiated to a solid hydrogen target (SHT) (ϕ50 mm, 100 mm thickness) [13] located in the final focusing point at ZDS (F11). The energies of the secondary beams are close to $240A$ MeV at F11, as shown in Table I. Particle identification before

TABLE I. Measured total charge-changing cross sections σ_{cc} and deduced root-mean-square proton radii r_p in this study; root-mean-square matter radii r_m deduced from the previous studies are also shown.

	Energy (MeV/nucleon)	σ_{cc} (mb)	r_p (fm)	r_m (fm)
^{30}Ne	230	250 ± 13	2.78 ± 0.32	3.311 ± 0.034 [18]
^{32}Na	240	275 ± 6	2.91 ± 0.21	3.22 ± 0.11 [14]
^{33}Na	225	277 ± 27	2.95 ± 0.65	
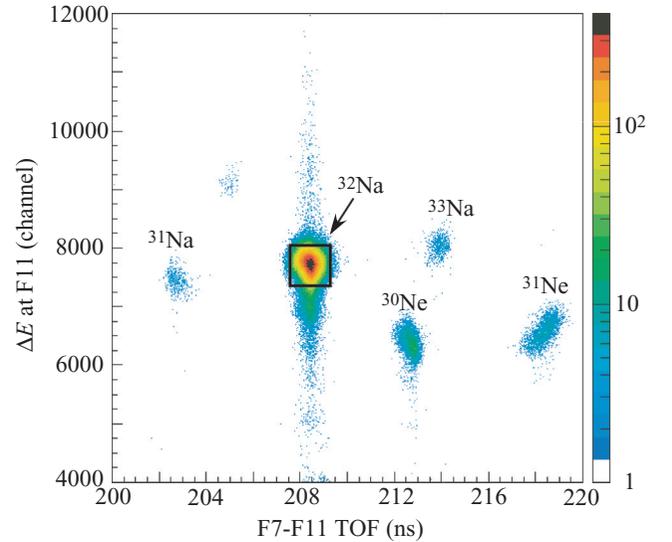
FIG. 2. (Color online) Typical particle-identification spectrum for ^{32}Na before a solid hydrogen target (SHT). The solid square shows the gate for selecting the events of ^{32}Na.

SHT has been done by ΔE-TOF measurements, where we measured the time of flight (TOF) between F7 and F11 using two plastic scintillators (3 mm thickness at F7 and 1 mm thickness at F11) and the energy-loss (ΔE) by a stack of four Si detectors (each 450 μm thickness) located at F11. A typical particle-identification spectrum before SHT is shown in Fig. 2, where a ^{32}Na beam was tuned to the center of Big-RIPS and ZDS. Downstream of SHT, a stack of three Si detectors (each 50×50 mm^2, 150 μm thickness) measured ΔE of the outgoing particles from SHT. The position and angle of the incoming particles to SHT were measured by two Parallel Plate Avalanche Counters (PPAC), located at F11. A typical ΔE spectrum after SHT, where we selected ^{32}Na before SHT inside the gate shown in Fig. 2 and averaged signals from three Si detectors, is shown in Fig. 3(a). The energy resolution of ΔE for $Z = 11$ is 2.8% in σ, and this resolution allows us to easily identify Z after SHT, as shown in Fig. 3(a).
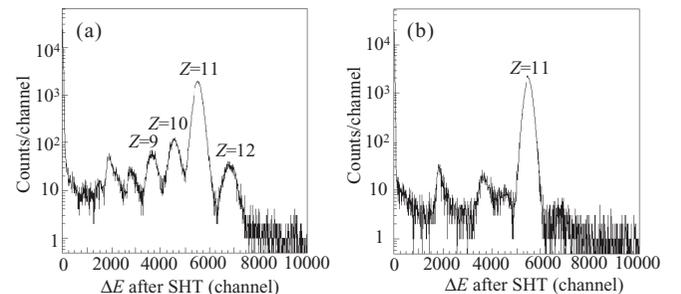
FIG. 3. (a) Typical ΔE spectrum for ^{32}Na measured by a stack of Si detectors located after the solid hydrogen target (SHT). Peaks for $Z = 9$, 10, 11, and 12 are clearly seen. (b) Same spectrum, but without SHT.

The principle of the experiment is the transmission method. σ_{cc} is derived from the equation

$$\sigma_{cc} = -\frac{1}{t}\ln\left(\frac{\Gamma}{\Gamma_0}\right), \qquad (1)$$

where Γ and Γ_0 represent the counting ratio of the particles for a target-in and target-out run, respectively, and t denotes the target thickness (i.e., the number of nuclei per unit area). To deduce Γ_0, we performed the measurement without solid hydrogen. The typical ΔE spectrum after the empty SHT, where the target cell remained, is shown in Fig. 3(b). In this spectrum, ^{32}Na was already selected by the gate in the ΔE-TOF spectrum. To deduce Γ's, the number of events were counted inside the ± 3.0 σ gate in the ΔE spectra when we fitted the peak of ^{32}Na ($Z = 11$) by a Gaussian. To verify the full transmission from SHT to the Si detectors located after SHT, we selected the position and the angle for the incoming nuclei using two PPAC located at F11. Γ and Γ_0 are 0.821 $\pm$ 0.007 and 0.948 $\pm$ 0.010, respectively, for ^{32}Na. It is noted that we did not see any channeling effects in the three Si detectors at F11, either with or without SHT. Thus, we did not make any corrections concerning the channeling. In Fig. 3(a), the peaks of events for the charge pick-up ($\Delta Z = +1$) and partial charge-changing ($\Delta Z = -1$ and -2) can be clearly seen. To deduce $\sigma_{\Delta Z=+1}$ and $\sigma_{\Delta Z=-1,-2}$, we counted the number of events inside the ± 3.0 σ gate for these peaks, where we used the same σ as that used in ^{32}Na ($Z = 11$). The length of the target cell of SHT was 100 mm. However, the target window (25 μm thickness Kapton) was expanded during the target production process. This surface expansion effect is well considered in Ref. [13]. Thus, upon considering the surface expansion, the SHT effective thickness was estimated to be 0.870 g/cm^2.

III. RESULTS AND DISCUSSION

A. Total charge-changing cross sections

The results of σ_{cc} are listed in Table I. The errors of σ_{cc} should be noticed. In Table I, only statistical errors are quoted since other sources of errors are negligible compared with this one. The target inhomogeneity is given as ± 0.3 mm in Ref. [13]. This corresponds to a $\pm 0.3\%$ uncertainty of the target thickness. The event selection condition in the ΔE-TOF and ΔE spectra might introduce an uncertainty in deducing σ_{cc}. This was confirmed to be less than $\pm 0.5\%$ by changing the gate width applied in the spectra.

To relate r_p from the observed σ_{cc}, we applied the method described in Refs. [7,8]. σ_{cc} is described by the following equation:

$$\sigma_{cc} = 2\pi \int b[1 - T^{P}(b)]\varepsilon(E)db, \qquad (2)$$

where b denotes the impact parameter, $T^{P}(b)$ is a part of the transmission function, and $\varepsilon(E)$ is the phenomenological correction factor at energy E [7]. In Refs. [7,8], $\varepsilon(E)$ for σ_{cc} with the carbon target has been introduced. In this experiment, the reaction target was the proton, and thus the same correction factor could not be applied. We made the correction factor for the proton target as follows. In previous studies, σ_{cc} for ^{12}C with the proton target have been investigated [2]. In Ref. [2], σ_{cc} with $296A$ MeV is available. By using the optical limit Glauber model, we deduced the correction factor so as to reproduce this observed σ_{cc}. In the present analysis, we assumed harmonic oscillator (HO) distributions for ^{12}C with the same parameters of HO for the proton and neutron distributions for ^{12}C. The parameters were fixed so as to reproduce the σ_{I} of ^{12}C + ^{12}C at relativistic energy [14]. A finite range parameter for the proton target has been introduced so as to reproduce the reaction cross section of p + ^{12}C at $231A$ MeV [15]. Thus, the obtained correction factor for the $296A$ MeV ^{12}C beam with the proton target is $\varepsilon(296) = 1.429 \pm 0.041$. We used this correction factor to apply the deduction of r_p for ^{30}Ne, ^{32,33}Na. We ignored any small differences of the beam energies, since in the carbon target the correction factor has only a slight energy dependence with 0.4% between the two energies ($296A$ and $240A$ MeV) [7]. To deduce r_p, we need to assume the shape of the point proton distributions. We used a two-parameter Fermi distribution for the proton distributions, which is given by

$$\rho(r) = \frac{\rho_0}{1 + \exp\left(\frac{r-R}{a}\right)}, \qquad (3)$$

where the half-density radius R and the diffuseness a should be determined. In this analysis, the diffuseness parameter a is fixed to be 0.6 fm. We adjusted only the radius parameter R so as to reproduce the observed σ_{cc}. The obtained r_p value for ^{30}Ne, ^{32,33}Na are also given in Table I.

For ^{32}Na, σ_{I} at relativistic energy was measured at GSI [16], and the RMS matter radius r_m deduced to be 3.22 ± 0.11 fm [14]. For ^{30}Ne, σ_{I} at $\sim 240A$ MeV was measured at Big-RIPS [17], and r_m deduced to be 3.311 ± 0.034 fm [18]. Therefore, our new proton radii enable us to derive the neutron radii of these nuclei. This can be done by employing the following relation:

$$r_m^2 = \frac{A}{Z}r_p^2 + \frac{N}{A}r_n^2, \qquad (4)$$

where r_n are the RMS neutron radii. The neutron skin thicknesses, $r_n - r_p$, for ^{30}Ne and ^{32}Na were calculated, and are 0.77 ± 0.36 and 0.46 ± 0.33 fm, respectively. In Fig. 4, the neutron skin thicknesses for Na isotopes [16] including the present ^{32}Na result (closed circle) are plotted against the difference of proton and neutron separation energies ($S_p - S_n$), which were calculated from the mass evaluated in Atomic Mass Evaluation 2012 (AME2012) [19]. The present result is consistent with the general trend of the skin thicknesses which correlate linearly with $S_p - S_n$. In relativistic mean-field calculations, the skin thicknesses of ^{30}Ne and ^{32}Na are 0.544 and 0.521 fm [20], respectively, which are also consistent with our deduced values.

B. Charge pick-up and partial charge-changing cross sections

In this experiment, charge pick-up, $\Delta Z = +1$, events were clearly observed, as shown in Fig. 3(a). For a comparison between the cases with and without SHT, we deduced $\sigma_{\Delta Z=+1}$, as shown in Table II for ^{30}Ne, ^{32,33}Na. According to Fig. 3, $\sigma_{\Delta Z=-1,-2}$ can be also easily deduced. Those cross sections for ^{30}Ne, ^{32,33}Na are given in Table II. The $\sigma_{\Delta Z=+1}$ values
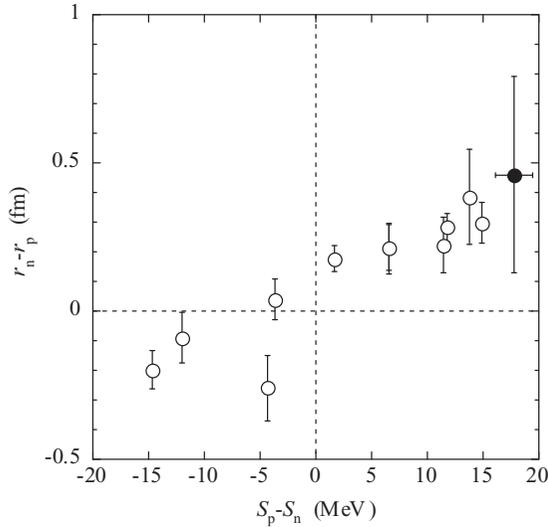
FIG. 4. Neutron skin thicknesses$(r_n - r_p)$ for Na isotopes as a function of the difference of the proton and neutron separation energies $(S_p - S_n)$ calculated from the mass evaluated in AME2012 [19]. Neutron skin thicknesses marked by the open circles obtained from Ref. [16] and the closed circle from the present study (^{32}Na).

are extensively studied using stable nuclei beams with various targets at various energies. For the relativistic energy region, the following empirical formula is given [21]:

$$\sigma_{\Delta Z=+1} = 1.7 \times 10^{-4} \gamma_{PT} A_P^2 \text{ (mb)}, \qquad (5)$$

where $\gamma_{PT} = A_P^{1/3} + A_T^{1/3} - 1.0$ and A_P and A_T are the projectile mass and the target mass, respectively. When we applied this equation to our cases, we obtained $\sigma_{\Delta Z=+1}$ = 0.5 to 0.6 mb for ^{30}Ne, ^{32,33}Na. The observed $\sigma_{\Delta Z=+1}$ are much larger by a factor of ∼100. According to Ref. [21], the deviation between the observed cross sections with stable nuclei and those calculated by Eq. (5) are within a factor of 2. Thus, this surprisingly large difference may reflect the exotic structure for neutron-rich unstable nuclei. According to Ref. [21], dependences of cross section for charge pickup on target mass are smooth from $A_T = 1$ to $A_T \sim 200$. However, it is known that the cross sections for (p, xn) reactions depend on the neutron/proton ratio of the nucleus that picks up charge. Thus, observed $\sigma_{\Delta Z=+1}$ with the proton target may be deviated from Eq. (5) in the unstable nuclei region. Further experimental and theoretical investigations are anticipated.

Charge-changing ΔZ dependences in the partial charge-changing cross sections for ^{30}Ne, ^{32,33}Na are shown in Fig. 5.

TABLE II. Measured charge-pickup cross sections $\sigma_{\Delta Z=+1}$ and partial charge-changing cross sections $\sigma_{\Delta Z=-1,-2}$ in this study.

	Energy (MeV/nucleon)	$\sigma_{\Delta Z=+1}$ (mb)	$\sigma_{\Delta Z=-1}$ (mb)	$\sigma_{\Delta Z=-2}$ (mb)
^{30}Ne	230	41.9 ± 3.3	109.4 ± 7.7	45.0 ± 3.6
^{32}Na	240	40.7 ± 2.2	114.0 ± 4.5	44.1 ± 2.1
^{33}Na	225	56 ± 13	116 ± 10	39.5 ± 6.0
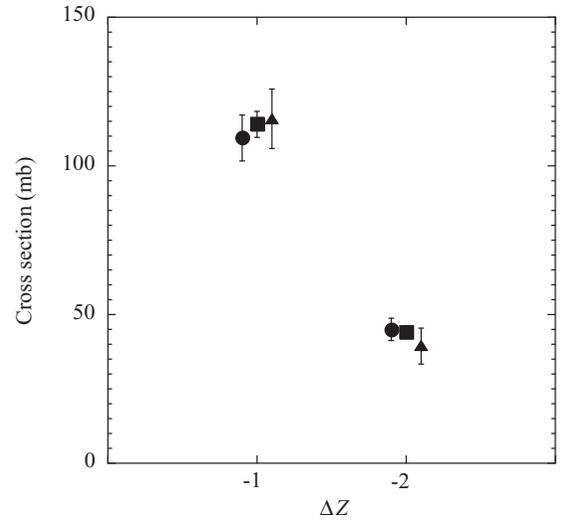
FIG. 5. Experimental partial charge-changing cross sections vs. charge changing ΔZ for ^{30}Ne (closed circle), ^{32}Na (closed square), and ^{33}Na (closed triangle), respectively.

In systematical measurements of partial charge-changing cross sections with stable nuclei, the general decrease in the cross sections with decreasing fragment charge is observed, except for nuclei with $N = Z$, where a strong odd-even effect is observed [22]. It seems that this general decrease holds even for very neutron-rich nuclei.

IV. SUMMARY

We measured the total charge-changing, charge pick-up, and partial charge-changing cross sections for ^{30}Ne, ^{32,33}Na with a proton target at ∼240A MeV. To deduce r_p from σ_{cc}, we applied the method introduced in Refs. [7,8] to deduce r_p from σ_{cc} with a proton target for the first time. The phenomenological correction factor in the Glauber model was introduced by using previously measured σ_{cc} for p+^{12}C at 296A MeV; this factor was applied to deduce r_p from the measured σ_{cc}. In ^{30}Ne and ^{32}Na, we deduced the neutron skin thickness by coupling with r_m deduced from σ_I at the relativistic energy. Although the errors are large, the obtained neutron skin thicknesses are almost similar to that of ^{31}Na and those of theoretical calculations in relativistic mean-field theory. This gives additional evidence that the development of a thick neutron skin is a common feature in neutron-rich nuclei. In this study, it is also shown that the method used to deduce r_p from σ_{cc} can be applied even to σ_{cc} with a proton target. However, it is noted that this method should be tested systematically on less exotic nuclei with the proton target. Further experimental investigations are anticipated. We observed a surprisingly large $\sigma_{\Delta Z=+1}$ for ^{30}Ne, ^{32,33}Na. The cross sections are much larger than the systematics deduced in stable nuclei. The observed charge-changing dependences in partial charge-changing cross sections show a general decrease in the cross sections with decreasing fragment charge, which is commonly observed in stable nuclei, except for nuclei with $N = Z$.

[1] H. Iwase, K. Niita, and T. Nakamura, J. Nucl. Sci. Technol. **39**, 1142 (2002).

[2] W. R. Webber, J. C. Kish, and D. A. Schrier, Phys. Rev. C **41**, 520 (1990).

[3] W. R. Webber *et al.*, Astrophys. J. **508**, 940 (1998).

[4] C. Zeitlin *et al.*, Phys. Rev. C **77**, 034605 (2008).

[5] L. V. Chulkov *et al.*, Nucl. Phys. A **674**, 330 (2000).

[6] O. V. Bochkarev *et al.*, Euro. Phys. J. A **1**, 15 (1998).

[7] T. Yamaguchi *et al.*, Phys. Rev. C **82**, 014609 (2010).

[8] T. Yamaguchi *et al.*, Phys. Rev. Lett. **107**, 032502 (2011).

[9] T. Suda *et al.*, Phys. Rev. Lett. **102**, 102501 (2009).

[10] http://www.gsi.de/fair/experiments/elise/index_e.html.

[11] K. Oyamatsu and K. Iida, Prog. Theor. Phys. **109**, 631 (2003).

[12] T. Kubo *et al.*, Nucl. Instrum. Methods B **204**, 97 (2003).

[13] T. Moriguchi *et al.*, Nucl. Instrum. Methods A **624**, 27 (2010).

[14] A. Ozawa *et al.*, Nucl. Phys. A **693**, 32 (2001).

[15] P. U. Renberg *et al.*, Nucl. Phys. A **183**, 81 (1972).

[16] T. Suzuki *et al.*, Phys. Rev. Lett. **75**, 3241 (1995).

[17] M. Takechi *et al.*, Phys. Lett. B **707**, 357 (2012).

[18] M. Takechi *et al.* (private communication) [Phys. Rev. C (to be published)].

[19] M. Wang *et al.*, Chinese Phys. C **36**, 1603 (2012).

[20] L. S. Geng *et al.*, Nucl. Phys. A **730**, 80 (2003).

[21] Ren Guoxiao, P. B. Price, and W. T. Williams, Phys. Rev. C **39**, 1351 (1989).

[22] C. N. Knott *et al.*, Phys. Rev. C **53**, 347 (1996).